P H Y S I C A L   R E V I E W   L E T T E R S

Nontouching Nanoparticle Diclusters Bound by Repulsive and Attractive Casimir Forces

Alejandro W. Rodriguez,[1] Alexander P. McCauley,[1] David Woolf,[2] Federico Capasso,[2]
J. D. Joannopoulos,[1] and Steven G. Johnson[3]

[1]*Department of Physics, Massachusetts Institute of Technology, Cambridge, Massachusetts 02139, USA*
[2]*Department of Applied Physics, Harvard University, Cambridge, Massachusetts 02139, USA*
[3]*Department of Mathematics, Massachusetts Institute of Technology, Cambridge, Massachusetts 02139, USA*

We present a scheme for obtaining stable Casimir suspension of dielectric nontouching objects immersed in a fluid, validated here in various geometries consisting of ethanol-separated dielectric spheres and semi-infinite slabs. Stability is induced by the dispersion properties of real dielectric (monolithic) materials. A consequence of this effect is the possibility of stable configurations (clusters) of compact objects, which we illustrate via a molecular two-sphere dicluster geometry consisting of two bound spheres levitated above a gold slab. Our calculations also reveal a strong interplay between material and geometric dispersion, and this is exemplified by the qualitatively different stability behavior observed in planar versus spherical geometries.

Electromagnetic fluctuations are the source of a macroscopic force, the Casimir force, between otherwise neutral objects [1–3]. In most geometries involving vacuum-separated metallic or dielectric objects (with a separating plane), the force is attractive and decaying as a function of object separation, and may contribute to "stiction" in microelectromechanical systems [4]. A repulsive interaction would be desirable to combat stiction as well as for frictionless suspension and other applications. Repulsive Casimir forces occur in a variety of settings, including theoretical magnetic materials [5], fluid-separated dielectrics [6,7], interleaved metallic geometries [8], and have also been suggested for composite metamaterials [9] (although repulsion with physical metamaterials has not yet been clearly demonstrated, as discussed below). In this Letter, we demonstrate stable Casimir suspension of realistic dielectric or metallic objects immersed in a fluid. Unlike previous work [10], this suspension does not involve one object enclosing another, but instead occurs between objects on opposite sides of an imaginary separating plane. This effect is a consequence of material dispersion, and is here validated in various experimentally accessible geometries consisting of ethanol-separated dielectric spheres and semi-infinite slabs. Furthermore, we show the possibility of achieving Casimir "molecular" clusters in which objects can form stable nontouching configurations in space—this is illustrated in a "diatomic" or "dicluster" geometry involving two dielectric spheres of different radii bound into a nontouching pair and levitated above a gold slab. Finally, our calculations reveal interesting effects related to the interplay of geometric and material dispersion, in which stability responds to finite size in a way that is qualitatively different in planar vs spherical geometries.

Casimir stability has been previously studied in at least four different contexts: first, in geometries involving mutually enclosed fluid-separated objects, in which the inner object is repelled by the outer object [10]; second, a slab-sphere geometry in which fluid-induced repulsion counteracts the force of gravity [11]; third, interleaved structures like the zipper geometry of [8], in which the surfaces of two complicated objects interleave so that their mutual attraction acts to separate the objects; and fourth, metamaterial proposals [9] that currently have no clear physical realization. The first two approaches (involving fluids) are illustrated by the schematics in Figs. 1(a) and 1(b). While all of these examples clearly demonstrate the possibility of Casimir stability, they leave something to be desired: they are limited to enclosed or complex geometries or require that stability lie only along a single direction (e.g., direction of gravity). It has been suggested that vacuum-separated chiral metamaterials may exhibit repulsive interactions and stable repulsive-attractive transitions [9], although no specific metamaterial geometries (chiral or otherwise) exhibiting repulsion have yet been proposed—in any case, the predicted chiral repulsive forces arise only for small separations where the metamaterial approximation cannot be trusted, and recent exact calculations indicate that they appear to be attractive [12]. Moreover, recent theoretical work has shown that vacuum-separated objects can never form stable configurations [13]. A less con-
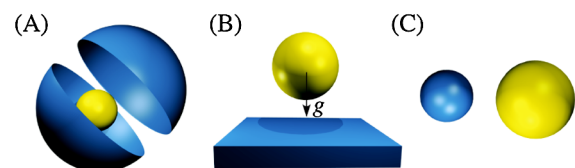

FIG. 1 (color online). Schemes for stable suspension of fluid-separated objects, involving: (a) enclosed geometries; (b) gravity countering Casimir repulsion; and (c) material dispersion producing repulsive *and* attractive Casimir forces (here).

strained and previously unexplored form of stability is one involving compact objects on either side of an imaginary separating plane, as illustrated in Fig. 1(c) for two spheres: in this case (involving fluids), we will show that the objects form stable configurations that are independent of external forces, and seem more accessible to experiment, opening up new possibilities for the creation of multibody clusters based on the Casimir force.

The Casimir force between two dielectric objects embedded in a fluid can become repulsive if their dielectric permittivities satisfy:

$$\varepsilon_1(i\xi) < \varepsilon_{\text{fluid}}(i\xi) < \varepsilon_2(i\xi), \tag{1}$$

over a sufficiently wide range of imaginary frequencies ξ [6]. The possibility of stable separations arises if the force transitions from repulsive at small separations (conceptually dominated by large-ξ contributions) to attractive at large separations (conceptually dominated by small-ξ contributions). A criterion for obtaining stability is therefore that Eq. (1) be violated at small ξ, and satisfied for $\xi > \xi_c$, with the transition occurring at some critical $\xi_c \sim 2\pi c/\lambda_c$ roughly related to the length scale λ_c at which the repulsive-attractive transition occurs. This criterion is only heuristic, but helps guide our intuition. The real system is more complicated, as we shall see, because the sign of the force also depends on many other factors such as the relative strength of the contributions of different frequencies (related to the strength of the ε contrast) as well as on finite-size effects.

After considering a number of possibilities, we have identified several material combinations that satisfy Eq. (1) for large ξ (small separations). Figure 2 (top) plots the dielectric permittivity $\varepsilon(i\xi)$ of various materials (Si, Teflon, SiO_2, and ethanol) satisfying Eq. (1) over some large range of ξ. In order to establish the existence of stable separations, we first compute the force between semi-infinite slabs separated by ethanol, using the Lifshitz formula [2]. Figure 2 (bottom) plots the Casimir force between semi-infinite slabs for different material arrangements, normalized by the corresponding force between perfectly-metallic slabs. Our results show that both Teflon-Si (red) and SiO_2-Si exhibit stable equilibria at $d_c \approx 120$ nm and $d_c^{(s)} \approx 90$ nm, respectively. SiO_2-Si exhibits a finite region of stability coming from the existence of an *unstable* equilibrium at a smaller $d_c^{(u)} \approx 29$ nm, a consequence of its two dielectric crossings $\xi_c^{(1)} \approx 2.62\pi c/\mu$m and $\xi_c^{(2)} \approx 26.42\pi c/\mu$m labeled in Fig. 2 (top). As mentioned above, this prescription for obtaining stability is only heuristic: for example, the force between Teflon-SiO_2 slabs is always attractive, even though their permittivities satisfy Eq. (1) at large ξ. In that case, while there is a crossing of the form of Eq. (1) at $\xi_c^{(2)}$, the repulsive contributions coming from $\xi > \xi_c^{(2)}$ are overwhelmed by the attractive contributions coming from $\xi < \xi_c^{(2)}$, since SiO_2 and Teflon become transparent at relatively
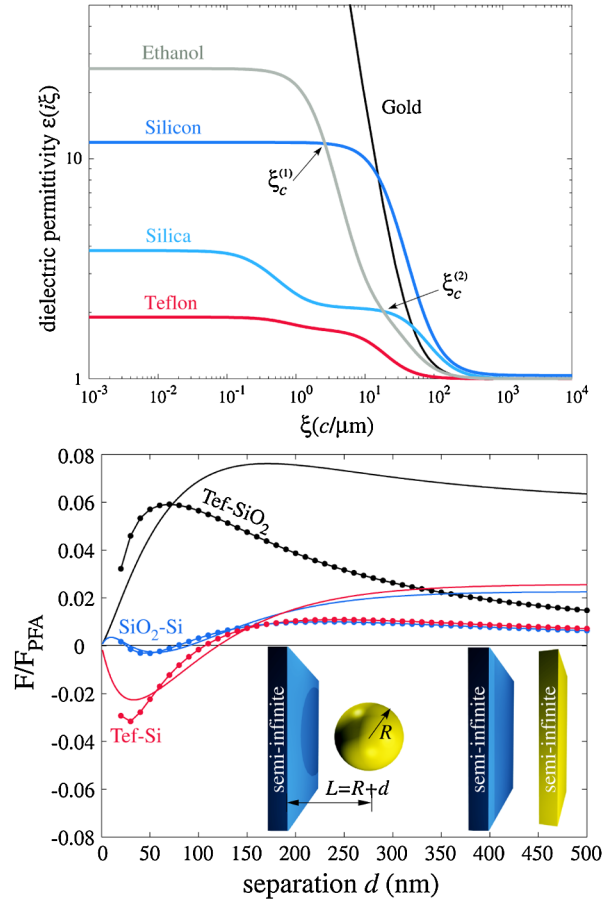

FIG. 2 (color online).   (Top): Plot of the dielectric permittivity $\varepsilon(i\xi)$ of various materials evaluated at imaginary frequency ξ (units of $c/\mu m$). (Bottom): Casimir force between a semi-infinite slab and a sphere (dots) and Casimir pressure between semifinite slabs (lines), normalized by the corresponding perfect-metal PFA force $F_{\text{PFA}} = \hbar c \pi^3 / 360 d^3$ (slab-sphere) and pressure $F_{\text{PFA}} = \hbar c \pi^2 / 240 d^4$ (slab-slab). The normalized force is plotted for various material configurations, described in the text.

small ξ. Thus, the repulsive region of the frequency spectrum merely *reduces* the attractive force between the objects at small separations.

We now investigate suspension of finite-size objects. For slab-sphere and sphere-sphere geometries, rapid exact calculations are performed using the spherical-harmonic scattering formulation of [14,15]. Given the material properties, the scattering-matrix formulation (derived from a path-integral evaluation of the Casimir energy) yields the exact Casimir force, with the only approximation being the numerical truncation of the sum over spherical-harmonic contributions—these contributions decay exponentially fast, and we only required harmonics up to order $\ell = 20$ to obtain better than 1% accuracy at relevant separations. For convenience, we evaluated the force at zero temperature T; because the room-temperature Matsubara wavelength $\hbar c/kT \sim 7.6 \mu$m is much larger than the <200 nm separations considered here, the finite-temperature corrections to the equilibrium separations are

small [2], e.g. $\ll 1\%$ for the $R_S = 100$ nm Teflon-Si sphere-sphere case in Fig. 4. Intuitively, one might expect the finite size or thickness of an object to suppress the contributions from small ξ (large "wavelengths"), and therefore to change (or eliminate) the separation at which the repulsive-attractive transition occurs. Here, where attraction comes from small-ξ contributions, one might expect the finite size to decrease the attractive contributions and therefore increase the equilibrium separation d_c.

Figure 2 (bottom) plots the force between a sphere of radius $R = 200$ nm and a semi-infinite slab for different material arrangements, normalized by the corresponding perfect-metal proximity-force approximation (PFA) force. (When referring to a geometry consisting of a semi-infinite α and finite β object, we shall denote the combination by α-β.) The results in this slab-sphere geometry look qualitatively similar to those in the slab–slab structure. In particular, both Teflon-Si and $SiO_2 - Si$ exhibit stable equilibria at $d_c \approx 105$ nm and $d_c \approx 78$ nm, respectively, roughly 15 nm smaller than the d_c in the slab-slab case.

The fact that d_c is smaller in the slab-sphere case than for semi-infinite slabs was initially unexpected since it contradicts the intuition described above. However, when we plot d_c for the various materials (solid dotted lines) as a function of $R \in (0, 350)$ nm in Fig. 3, we indeed observe the expected behavior: as R decreases, d_c increases, asymptoting to a constant at $R = 0$ that corresponds to the Casimir-Polder force between a spherical nanoparticle and a slab [14]. Similar increases in d_c as thickness t is decreased are observed in *some* of the finite-slab geometries (solid lines) in Fig. 3, at least in all of the configurations where the thickness of the silicon is varied. In the $t \to \infty$ limit for the slab-slab case, the semi-infinite result is recovered. For the slab-sphere case with $R \to \infty$, the asymptotic d_c occurs for a smaller separation than for semi-infinite slabs: in this limit, where PFA is valid, the curvature of the spheres yields an average separation that is larger than d_c.

An interesting question is to what extent one may tailor object geometries in order to change the qualitative features of the force, e.g., its sign. With this question in mind, the dashed lines in Fig. 3 show d_c for slab-slab geometries in which the two solid materials have been exchanged so that the finite-thickness slab is no longer silicon. Apparently, changing which slab is finite qualitatively reverses the dependence on d_c in some cases: for Si-Au and Si-SiO_2 slabs, the equilibrium separation d_c *decreases* with decreasing thickness t, corresponding to an *increased* attractive force despite the fact that the attractive contributions arise from small ξ (which are intuitively cut off by the finite thickness). This reversal, however, does not happen in all cases: it does not occur for the Si-Teflon slab-slab geometry or for *any* of the slab-sphere geometries (and we do not plot d_c in these reversed cases because the results are very similar to the original results). Evidently, the finite *lateral* size of the spheres has a dramatic qualitative interaction with the material dispersion. In future work, we plan
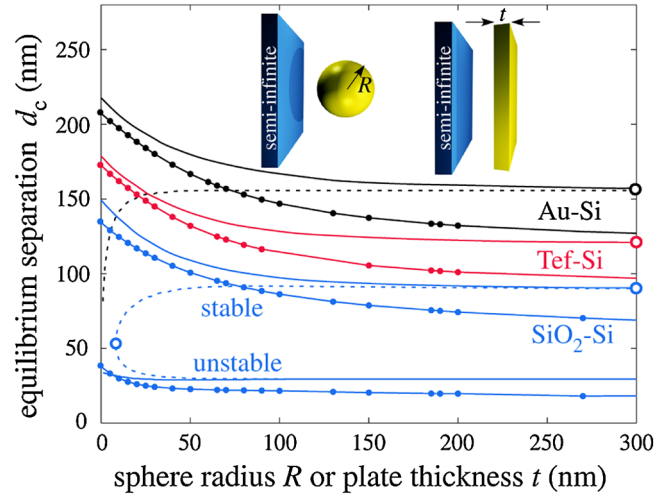

FIG. 3 (color online). Equilibrium separation d_c vs sphere-radius (R) or slab-thickness (t) for various slab-sphere (dots) and slab-slab (lines) configurations. Dashed lines correspond to slab-slab geometries with materials swapped (semi-infinite silicon slab).

to investigate this interesting interplay between material and geometric dispersion, in addition to the finite-size behavior exhibited by the finite gold [16] and SiO_2 slabs.

Another feature worth noting in Fig. 3 also stems from the anomalous response of the Si-SiO_2 slab-slab geometry to changes in the SiO_2 thickness t: the stable $d_c^{(s)}$ and unstable $d_c^{(u)}$ equilibria bifurcate at a radius R_c, below which the force is purely attractive at all d.

In what follows, we illustrate an interesting corollary of this type of stability: the possibility of obtaining stable noncontact configurations of compact objects at a nonzero separation. In particular, we calculate the Casimir force in a nanoparticle-dicluster system consisting of Teflon and silicon spheres, of different radii R_T and R_S, respectively, immersed in ethanol. The force F_{SS} between the spheres is plotted in Fig. 4 (bottom) for different sets of radii $R_S = \{99.69, 293.67, 368.39\}$ nm   and $R_T = \{262.09, 32.67, 176.64\}$ nm, respectively. This choice of the radii was motivated by one possible experimental configuration, in which the pair of spheres are also levitated above a planar slab: in this geometry, discussed below, the sphere radii are chosen so that both spheres are suspended at the same height above the slab. With this choice of materials, the spheres exhibit a stable (orientation-independent) surface-surface equilibrium in the 100–150 nm range.

To make such a dicluster pair easier to observe in experiments, one could simultaneously suspend them at a known distance above a planar substrate, using the interplay between the repulsive Casimir force and gravity to create stable levitation. For simplicity, we investigate this possibility within the additive approximation: the slab-sphere and sphere-sphere interactions are considered independently. Because Casimir forces are not additive, the presence of the slab will change the stable separation of the
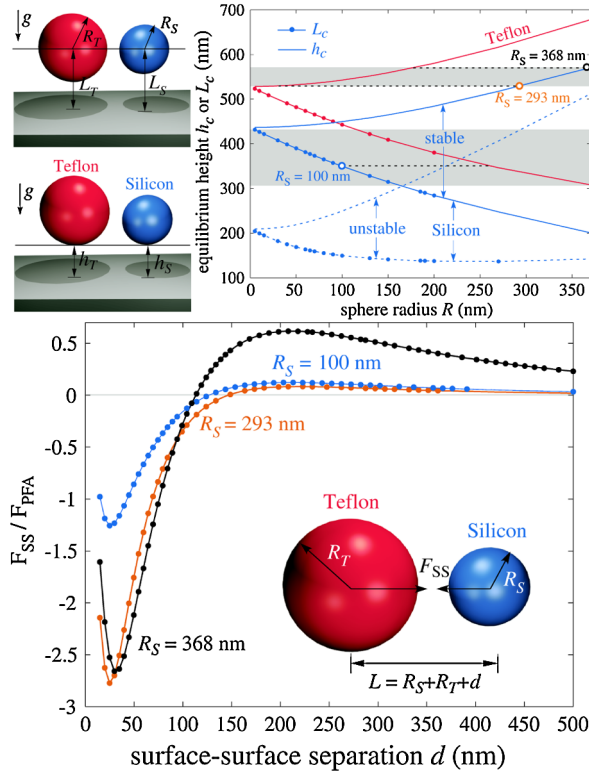
FIG. 4 (color online). (Top:) Plot of the stable equilibrium center-surface (L_c) and surface-surface (h_c) separation between either a Teflon (red) or silicon (blue) sphere and a semi-infinite gold slab (depicted schematically on the left inset), as a function of sphere-radius R. The black lines also show the presence of an unstable equilibrium in the silicon-sphere case. (Bottom:) Plot of the force F_{SS} between two Teflon and silicon spheres of radii R_T and R_S, showing the existence of a stable equilibrium.

spheres (and vice versa for the stable height of the spheres). However, this approximation forms a useful starting point for the design of such an experiment and should even be accurate in the limit where the sphere diameter is much larger than the stable surface-surface separations (here, most of the diameters are at least twice the stable separations). Figure 4 (top) shows a plot of the equilibrium surface-surface (h_c) and center-surface ($L_c = h_c + R$) separations of the Teflon (red) and silicon (blue) spheres suspended above a semi-infinite gold slab, as a function of sphere radius R. As shown by the figure, decreasing R acts to increase L_c and decrease h_c. The decrease in h_c occurs much more rapidly than in Fig. 3 due to the fact that, in addition to geometric dispersion, the force of gravity scales as the mass ρV of a sphere (where the density $\rho \approx \{2330, 2200, 789\}$ kg/m^3, for {Si, Teflon, ethanol}, respectively). The center-center separation $L_c = h_c + R$ increases with increasing R because $\partial h_c / \partial R > -1$. In addition to a stable equilibrium h_c, Au-Si exhibits an unstable equilibrium at smaller d_c due to the transition to an attractive Casimir force for small separations; if the sphere were ever pushed below the unstable equilibrium

point, it would continue downward and adhere to the slab. This would be a concern for experiments if fluctuations in the sphere height could push it below the unstable equilibrium, but as seen from Fig. 4 the distance between the stable and unstable equilibria is over 200 nm for $R < 50$ nm nanoparticles.

The gray areas in Fig. 4 (top) depict regions in which the L_c or h_c of the two spheres can be made equal by an appropriate choice of radii, as shown schematically in Fig. 4 (top left). This determines the stable configuration of the two-sphere dicluster when they are brought together above the surface; the three dashed horizontal lines in Fig. 4 (top) correspond to the radii used for the force calculation in Fig. 4 (bottom).

[1] H. B. G. Casimir, Proc. K. Ned. Akad. Wet. **51**, 793 (1948).
[2] E. M. Lifshitz and L. P. Pitaevskii, *Statistical Physics* (Pergamon, Oxford, 1980), Part 2.
[3] K. A. Milton, J. Phys. A **37**, R209 (2004).
[4] H. B. Chan, V. A. Aksyuk, R. N. Kleinman, D. J. Bishop, and F. Capasso, Science **291**, 1941 (2001).
[5] T. H. Boyer, Phys. Rev. A **9**, 2078 (1974); O. Kenneth, I. Klich, A. Mann, and M. Revzen, Phys. Rev. Lett. **89**, 033001 (2002); F. S. S. Rosa, D. A. R. Dalvit, and P. W. Milonni, Phys. Rev. A **78**, 032117 (2008).
[6] I. E. Dzyaloshinskiĭ, E. M. Lifshitz, and L. P. Pitaevskiĭ, Adv. Phys. **10**, 165 (1961).
[7] J. Munday, F. Capasso, and V. A. Parsegia, Nature (London) **457**, 170 (2009).
[8] A. W. Rodriguez, J. D. Joannopoulos, and S. G. Johnson, Phys. Rev. A **77**, 062107 (2008).
[9] R. Zhao, J. Zhou, T. Koschny, E. N. Economou, and C. M. Soukoulis, Phys. Rev. Lett. **103**, 103602 (2009).
[10] A. W. Rodriguez, J. Munday, D. Davlit, F. Capasso, J. D. Joannopoulos, and S. G. Johnson, Phys. Rev. Lett. **101**, 190404 (2008); S. J. Rahi and S. Zaheer, Phys. Rev. Lett. **104**, 070405 (2010).
[11] A. P. McCauley, A. W. Rodriguez, J. D. Joannopoulos, and S. G. Johnson, Phys. Rev. A **81**, 012119 (2010).
[12] A. P. McCauley *et al.* (to be published).
[13] S. J. Rahi, M. Kardar, and T. Emig, arXiv:quant-ph/0911.5364v1.
[14] S. J. Rahi, T. Emig, N. Graham, R. L. Jaffe, and M. Kardar, Phys. Rev. D **80**, 085021 (2009).
[15] A. Canaguier-Durand, P. A. Maia Neto, I. Cavero-Pelaez, A. Lambrecht, and S. Reynaud, Phys. Rev. Lett. **102**, 230404 (2009).
[16] A. Lambrecht, I. Pirozhenko, L. Duraffourg, and P. Andreucci, Europhys. Lett. **77**, 44 006 (2007).